

Interaction of terahertz radiation with composites based on track membranes with oriented metal nanowires

© G.V. Gorokhov,¹ D.L. Zagorskiy,² N.I. Valynets,¹ A.V. Melnikov,¹ I.M. Doludenko,²
V.M. Kanevskiy,² S.A. Maksimenko¹

¹ Institute for Nuclear Problems of Belarusian State University,
220006 Minsk, Belarus

² Kurchatov Complex Crystallography and Photonics, NRC „Kurchatov Institute“,
123182 Moscow, Russia
e-mail: gleggorokhov@yandex.ru

Received October 6, 2025

Revised November 21, 2025

Accepted November 27, 2025

Electromagnetic properties of composites fabricated by matrix synthesis consisting of arrays of oriented nanowires with varying geometries embedded within growth matrices — polymer track-etched membranes — have been investigated in the terahertz frequency range. For these composites, a dependence of the transmission coefficient T of polarized terahertz radiation has been observed on both the angle between the nanowire inclination direction within the matrix and the electric field vector E , as well as on the geometric parameters of the nanowires. This dependence is shown to be determined by the nanowire tilt angle and the formation of an anisotropic percolation network within the composite. A model describing the development of such a percolation network as a function of the nanowire array geometry has been proposed.

Keywords: composite materials, track-etched membranes, metal nanowires, terahertz radiation, radiation polarization.

DOI: 10.61011/TP.2026.04.63264.274-25

Introduction

The synthesis and systematic investigation of novel nanomaterials, as well as the composites and nanostructures derived from them, are of considerable theoretical and practical interest. The metal nanowires (NWs) characterized by their nanoscale diameter and elongated morphology represent a promising class of nanomaterials. One of the methods of NWs production is matrix synthesis, i.e. filling a porous matrix with a desired material. The main advantage of this method is the precise matching of geometrical parameters of the produced nanoparticles with the shape of matrix pores, which provides homogeneity and reproducibility of the geometrical parameters [1].

In addition to porous anodic aluminum oxide (AAO) [2,3], track-etched membranes (TMs) can serve as effective templates for nanomaterial fabrication. These membranes represent thin polymer films featuring through-pores with a stochastic spatial distribution, fabricated via irradiation with heavy ions followed by chemical etching of the resulting latent damage tracks [4,5]. Filling the pores with the required substance can produce both a polymer composite material (PCM) that contains nanowires as inclusions as well as free-standing nanowires designed for constructing polarizers [6] and as nano-actuators [7].

Unique geometry of the NW arrays produced by the matrix method determines a wide spectrum of possible applications. For instance, a small curvature radius of NW ends makes it possible to use them as field emission

cathodes for emission of electrons or heavy ions. A developed surface of the array enables its use as catalysts, heatsinks as well as substrates for surface-enhanced Raman spectroscopy (SERS) [8].

Adjustability of the NW composition makes it possible to specify electric and magnetic properties of the composite. A stochastic nature of the TM pores distribution makes it possible to use the nanowires made of ferromagnetic materials for data encryption (nanobarcoding) [9]. Creating heterojunctions inside the nanowires by alternating electrodeposition of thin layers of the magnetic and nonmagnetic materials enables the manufacturing of field sensors that use the gigantic magnetoresistance effect as well as generating THz radiation when a current is passed through the array of the nanowires that contain heterojunctions between the various magnetic layers [10]. An inverse problem of detecting THz radiation by means of the nanowires is of high interest as well.

The track-etched membranes are characterized by adjustability of the geometric parameters of the pores at the production stage, while the AAO pores are limited by hexagonal geometry and parallelism [11]. Thus, a density of the pores and their spatial orientation (inclination and its spread) can be specified at the irradiation stage, whereas their shape (cylindrical, conical, biconical) is determined at the etching stage. That enables the fabrication of the arrays of oriented structures (nanowires, nanotubes, nanocones) with a specified geometry and density. The nanowires and the polymer composites, produced this way, possess an

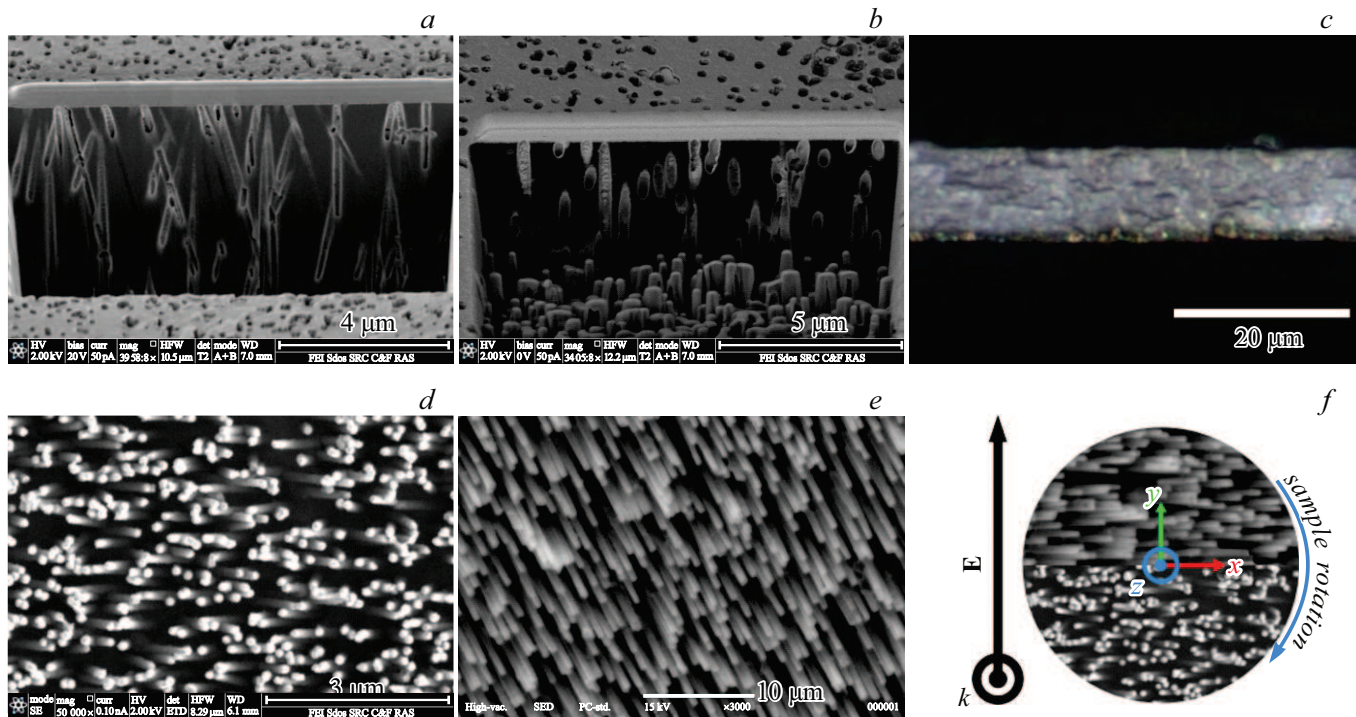


Figure 1. SEM images of the R (*a*) and U-type (*b*) TMs cross-sections; *c* — the optical image of a cleavage of PCM containing ONWA of $\sim 1 \mu\text{m}$ height; SEM images of 100 nm diameter nanowire (NW) arrays after removal of R-type (*d*) and U-type (*e*) templates; *f* a scheme of the sample placement in a THz spectrometer.

anisotropy of electromagnetic properties and, therefore, are promising for some application fields, including UHF and terahertz engineering [12,13].

It is well established that composite materials incorporating randomly distributed electrically conductive [12,14] and ferromagnetic nanoscale inclusions are of considerable interest for broadband electromagnetic interference (EMI) shielding. Leveraging these composites, active research efforts are focused on developing scalable fabrication technologies for compact microwave (MW) and terahertz (THz) devices.

It can be assumed that certain ordering of the composite structure, which is achieved in PCM, will additionally enable creating such terahertz optics devices as polarizers, attenuators and filters. In this context, the investigation of interaction effects between terahertz (THz) radiation and arrays of oriented nanowires (Oriented-Nanowire Array, ONWA) of various types is of considerable scientific interest and constitutes the focus of the present study.

1. Experimental

In the present study, three types of track-etched membranes fabricated at the Joint Institute for Nuclear Research (JINR, Dubna, Russia) were employed. These membranes feature distinct distributions of pore inclination angles, which were predefined during the heavy-ion irradiation stage; their key parameters are summarized in Table. All

the membranes had the thickness of $\sim 12 \mu\text{m}$. The first type of the matrices is referred as „randomly inclined“ or R geometry (Fig. 1, *a*) possess a spread of the pore inclination angle in one plane within the range of $\pm 30^\circ$, while in a perpendicular direction the angle varies by no more than 0.5° . The second type of TMs possesses mutually parallel pores that are oriented normal to the membrane plane (hereinafter referred to as „vertical“ or V). The pores of the third type of membranes (referred to as „uniformly inclined“ or U) are also mutually parallel, but inclined to the membrane surface at the angle of 43.5° (Fig. 1, *b*). The table also provides values of the pore diameter d , the pore density n (a number of pores per unit area of the TM) and porosity $n_p = n\pi d^2/4$ that is calculated for cylindrical pore without taking into account their inclination and intersection.

Further, we will designate the membranes as Xd , where X means the membrane type (R, V and U), while d is a diameter of its pores in nanometers. Composites based on such TMs will be designated as $Xd-H$, where H is an ONWA height in microns.

The above-described membranes were used to produce the polymer composite materials containing the nanowires that are made of the $\text{Fe}_{0.2}\text{Ni}_{0.8}$ permalloy and grown in the TM pores. The nanowires were grown using the electrical deposition method, which standard procedure (including a two-component electrolyte and two-electrode galvanic process scheme) is described in the study [15]. The soft magnetic permalloy was selected to be a material for the

Types of investigated track membranes

TM designation	R30	R65	R100	V100	U500
Pore geometry	$\pm 30^\circ$	$\pm 30^\circ$	$\pm 30^\circ$	0°	43.5°
d of pores, nm	30	65	100	100	500
Pore density n , cm^{-2}	$9.1 \cdot 10^9$	$4.5 \cdot 10^9$	$1.2 \cdot 10^9$	$5 \cdot 10^8$	$4.8 \cdot 10^7$
Porosity n_p , %	6.4	14.9	9.4	3.9	9.4

nanowires due to prospects of affecting its electromagnetic properties with a constant magnetic field [2], which are, however, beyond the scope of the present study.

Both the initial matrices as well as the produced nanowires were studied by the method of Scanning Electron Microscopy (SEM, the JEOL JSM microscope), which operated in a secondary electron mode. The pore structure of the initial matrices was studied on their metallized cleavage (Fig. 1, *a, b*), while the ONWAs themselves were studied after removal of the matrix. The obtained images of the arrays of the nanowires for the samples R and U are shown in Fig 1, *d, e*, respectively. The images of the pore channels and the arrays of the nanowires produced on their basis demonstrate the match between their parameters (diameters and inclinations).

A length of the nanowires in the composites L , which is determined by the time of electrical deposition, was characterized by analysis of an optical image of an end-face surface of the composite transect by means of the microscope (Fig. 1, *c*) taking into account an assumption that the NW array's height observed on the optical image for the samples of the R series is equal to the length of the nanowires. For the samples of the R series, the length of the nanowires varied within the range 1–8 μm .

The transmittance of the composites containing NWs was measured within the range 0.1–1 THz by means of the time-domain terahertz spectrometer EXPLA T-spec with linearly polarized incident radiation. A direction of the electric vector E is fixed. Therefore, in order to measure the dependence of the transmittance T on polarization of incident THz radiation, the sample was placed on a graduated rotary platform in a plane normal to the direction of propagation of radiation (the z axis of the film, around which the sample is rotated during measurements, coincides with the k direction). Fig. 1, *f* shows spatial orientation of the studied composite sample with the nanowires in relation to the direction of THz radiation propagation as well as a direction of NWs inclination: the x axis in the film plane corresponds to the direction of maximum inclination of the nanowires (± 30 or 43.5°), while the y axis correspond to minimum inclination.

An angular dependence of the transmittance was measured with a step of 10° . When the rotary platform was rotated, an angle between the direction of polarization of the external field and the direction of NW inclination gradually

varied. The value of T for each angle was averaged by 32 measurements in order to improve a signal-to-noise ratio.

2. Results and discussion

Fig. 2 presents the angular dependences of the transmittance of linearly polarized THz radiation within the range of 0.1–1 THz for the samples with three different geometries. The transmittance T (Fig. 2, *a, c*) of the R-type and U-type composites exhibits a pronounced dependence on the sample orientation relative to the polarization direction of the incident THz radiation. Such an effect is attributed to the predominant inclination of the nanowires along one direction that coincides with the x axis in Fig. 1, *f*. As for any extended particles, an electromagnetic response (currents excited in particles by the external field) of the nanowires to the field directed along their axis is much higher than to the field directed perpendicularly. Thus, tilting the NWs along the polarization direction yields a non-zero field projection onto the NW axis, resulting in a pronounced electromagnetic response. In the case when polarization of the external field is directed perpendicular to the NW axis, the NW response turns out to be insignificant, thereby complying with observation of a zero degree of polarization $P = (T_{\max} - T_{\min}) / (T_{\max} + T_{\min})$ of the V-type samples. Difference between a longitudinal and a transverse electromagnetic response of the nanowires to the external field results in much higher values of transmittance T for the V-type samples as compared to the samples of the U-type and R-type.

Notably, for the composite U500-4 the polarization dependence of T is much less pronounced (Fig. 2, *c*) than for the R-type sample (Fig. 2, *a*), that possesses the polarization degree P (Fig. 2, *d*) of up to 90%, while for U-type composite it does not exceed 5%. Such difference in transmission of THz radiation through the samples based on the R-type and U-type membranes can be attributed to their structural differences. For the R-type composites, where a sufficient length of the nanowires leads to the intersections (and, therefore, electrical contacts — Fig. 1, *d*) between them, whereas in the U-type composites the nanowires will remain isolated regardless of the length (Fig. 1, *e*). The formation of the electrical contacts between inclusions in the composites, in turn, leads to the formation of a

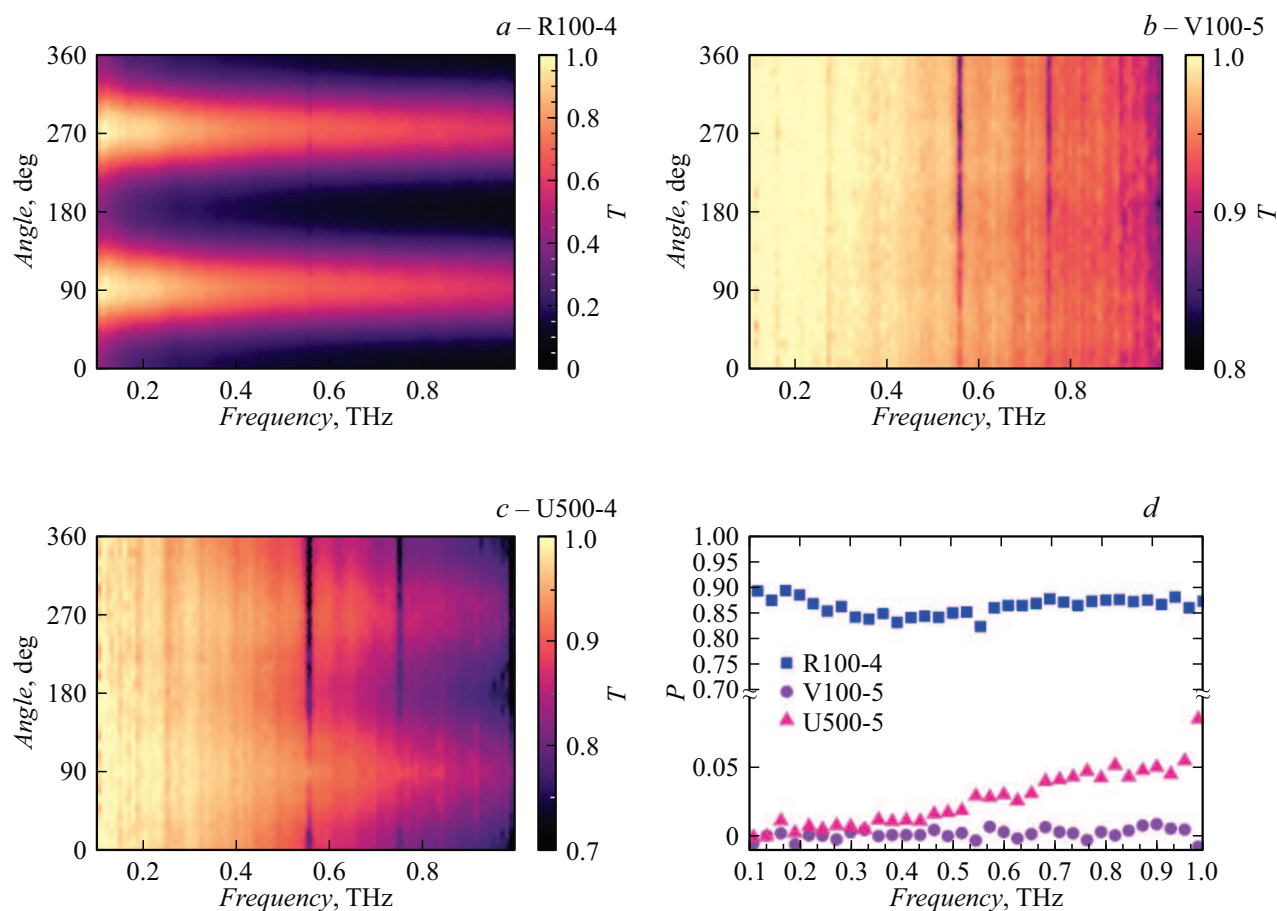


Figure 2. *a–c* — comparison of the dependence of the transmittance with the metal nanowires of various spatial orientation on polarization of incident radiation within the range of 0.1–1 THz; *d* is a degree of polarization for the respective samples. The angles 0° , 180° and 360° correspond to polarization of the external field $E \parallel x$, while the angles 90° and 270° correspond to polarization $E \parallel y$.

percolation network and, therefore, the emergence of static (DC) electric conductivity therein [16,17].

The values of the transmittance and the polarization degree observed for the R-type composites, indicate that they are promising for the THz polarizers production. This requires the optimization of both geometric parameters of the composite as well as materials included in the NW composition. Thus, the polarizers based on nematic liquid crystals are characterized by the relatively low maximum transmittance [18], that significantly limit their application despite high values of the extinction ratio $ER = 10 \log(T_{\max}/T_{\min})$. The extinction ratio value for the composites considered herein is ~ 10 –12 dB within the range 0.1–1 THz, which is close to values for the wire grid polarizers fabricated of carbon nanotubes [19]. However, the fabrication of this type of polarizer for the THz range entails certain technological difficulties [20].

In order to study the influence of percolation phenomena on transmission of THz radiation through the studied composites, we have considered the influence of the variation of the diameter and length of the nanowires to the frequency dependence of T for the R-type composites. Fig. 3 shows the frequency dependences of maximum and minimum T

that corresponds to the cases $E \parallel y$ and $E \parallel x$ (Fig. 1,*f*) for the composites of the R30, R65 and R100 series with the different NW length.

Two patterns are observed for all the considered series of the composites with the increasing NW length: 1) the substantial reduction of T within the entire range; 2) the suppression of the dependence of T on the frequency (of a frequency dispersion). The observation of these trends is attributed to the emergence of percolation effects in samples with varied pore inclinations as the nanowire (NW) length increases.

The essence of the percolation phenomenon lies in the formation of a macroscopic conductive pathway driven by physical contacts between filler particles. Within this percolating network, charge can be transferred between any pair of nanowires through a series of inter-particle junctions.

For the transmittance T of the samples R30-1, R65-2 and R100-3 (Fig. 2), which contain short nanowires, the highly pronounced frequency dispersion related to finite-length effects in single nanowires is observed. The finite-length effect consists in the polarization of particles in the external field [21] — the external field induces currents inside the particles, that result in accumulation of opposite charges at

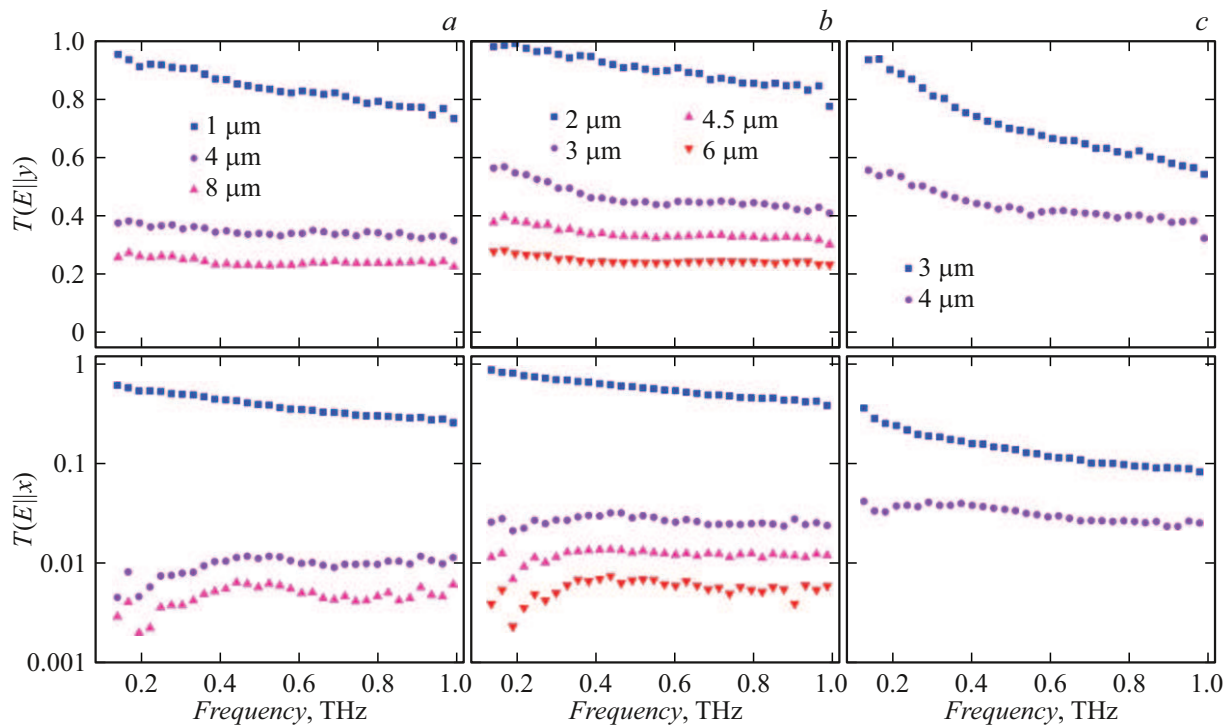


Figure 3. Transmittance values of the composites containing the nanowires of varied length and the diameters of 30 (a), 65 (b), 100 nm (c). The upper and lower rows correspond to maximum and minimum transmittance ($E \parallel y$ and $E \parallel x$, respectively).

opposite sides (along a longitudinal or transverse direction). These charges create the so-called depolarizing field that is directed opposite to the external field, which ultimately results in suppression of the entire field inside the particles as compared to the external field. As a result, the currents induced in the particle under an external field attenuate, thereby resulting in drop of the electromagnetic response of the particles, that, in its turn, is expressed in an increase in transmittance T of electromagnetic radiation through the sample. Since an effect of current reduction in the particles is frequency-dependent and increases with reduction of the external field frequency, electric conductivity of this composite is characterized by a reactive capacitance response that is similar to a series RC-circuit [22,23]. This explains reduction of T with an increase of the frequency (frequency dispersion), which is observed for the composites of V-type and U-type (Fig. 2, b, c), where nanowires do not contact each other, as well as for the R-type composites with a small NW length. Thus, presence of frequency dispersion of the electromagnetic response as well as the high values of T in all the considered spatial orientations indicate that the NW length in the samples R30-1, R65-2 and R100-3 is not enough for forming the continuous percolation network.

The increase of the nanowires length results in an increase of the number of physical contacts between them and gradual formation of the continuous percolation network of the nanowires across the entire volume of the sample. Simultaneously, the number of the isolated nanowires that can be polarized in the external field decreases to a negligible one. At the same time, the currents flowing

through the nanowires embedded in the percolation network are no longer suppressed by the finite-length effect, since presence of intersections between the nanowires allows the charges to flow between the nanowires.

It results in multiple reduction of the T values for both directions of the external field polarization, with the effect being more pronounced for $E \parallel x$ polarization. The abrupt reduction of the values of T is accompanied by significant reduction or even disappearance of frequency dispersion, which can also indicate suppression of the finite-length effects in the nanowires. Based on the experimental data shown in Fig. 3, we assume that a percolation transition for the samples R30 and R65 is observed at the NW length being in the range of 1–4 μm and 2–3 μm , respectively. At the same time, low frequency dispersion of T , which is observed for the R100-4 sample, makes it possible to assume that it either achieved percolation or a very slight increase of the NW length is required to achieve it. In order to confirm that for the considered samples the qualitative change of T spectra with increasing of the NW length is exactly related to the formation of the conductive percolation network therein, we provide ONWA modeling by the Monte Carlo method in order to determine the NW length, at which percolation is achieved.

3. Modeling

As it is shown above, the presence of percolation network in the considered composites results from the density of the

nanowires, their angular distribution, diameter and length, wherein all the parameters except for the last one are fixed at the TM production stage. That is why, it is advisable to investigate the development of the percolation phenomena in the composites under study, first of all, as a function of the NW length. In the studied case, this length acts as an analog of a percolation threshold. For theoretical study of the percolation phenomena in the ONWA composites, the Monte Carlo method was employed in order to model the film samples that contain 5000 nanowires. The cylindrical nanowires of the length L and the diameter d were generated in such a way that one of their ends had a coordinate $z = 0$ and was randomly placed within a range of $x \in [0, x_0]$ and $y \in [0, y_0]$. The sample had an area $S = x_0 \cdot y_0 = N/n$, where n is the pore density, N is the total number of the nanowires in the sample. The nanowires were generated with random inclination along the x axis within the range $\varphi \in [-30^\circ, 30^\circ]$ and zero inclination along the y axis, thereby corresponding to the experimental series of the R-type samples.

The criterion for electric contact between two nanowires was assumed to be an intersection of their cylindrical volumes, that corresponds to a case when a distance between the NW axes is smaller than their diameter. A condition of electric percolation achievement in the sample was assumed to be a presence of a continuous conductive path that connects nanowires at the sample edges that are opposite along the x axis, via a network of contacts between the nanowires. The more detailed description of a calculation method used in this study can be found in [24]. Our modeling considered the samples that were elongated along the x axis with an aspect ratio $x_0/y_0 = 10$, since the percolation network in the modeled system is predominantly developed along the direction of NW inclination [25]. For each set of the geometric parameters of the composite — the diameter and the length of the nanowires and the pore density — 10 random generations were performed; the percolation for these parameters was considered achieved if it was observed in 9 of 10 cases.

Fig. 4 shows the dependences of a theoretical estimation of the NW length L_p , at which percolation is achieved (i. e. the percolation threshold), on the pore density n for the three different diameters of the nanowires. The dependences for the diameters 30, 65 and 100 nm are evaluated for the pore density range that corresponds to TM porosity from 2.5% to 20%. It should be noted that although the full TM thickness is unvaried, the entire electromagnetic response of the composite is formed in an ONWA-filled layer of the thickness L_p , whose porosity is constant along the z axis. Thus, an occurrence of percolation can not be judged directly by porosity. However, its value is identically equal to a volume fraction of the nanowires in the composite and can be used for comparing the obtained results with composites produced by other methods, since, as a rule, the volume concentration of inclusions is associated with the percolation threshold determination.

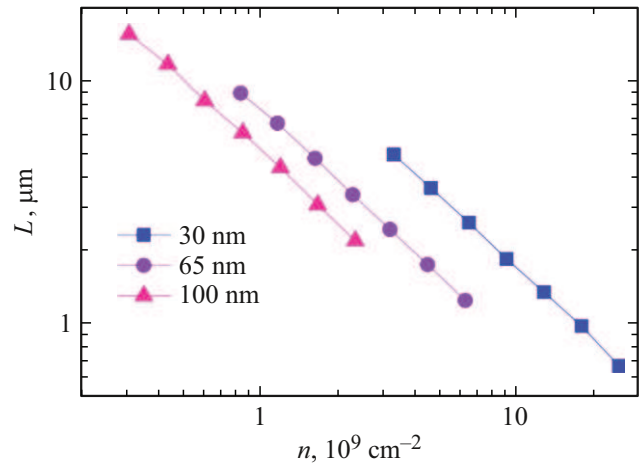


Figure 4. Dependences of the NW lengths L_p , at which percolation is achieved, on the pore density at the different diameters of the nanowires.

It is clear from Fig. 4 that the NWs length L_p , at which percolation is achieved, is inversely proportional to: 1) the pore density for the samples with the same NW diameter; 2) the NW diameter for the samples with the same pore density. The relatively smaller NWs length L_p required for achieving of percolation means that, practically, for these samples it is easier to achieve the percolation transition (a lower time of NWs growth is required and smaller limitations are imposed to a minimum thickness of the membrane), upon achievement thereof polarization characteristics are strongly improved. It is predicted by a theoretical model that for the series of the experimental samples R30-1, R65-2 and R100-3 percolation is achieved when $L_p = 1.85$, 1.75 and $4.4 \mu\text{m}$, respectively. Thus, the theoretical estimations of the length of percolation achievement are in good agreement with the experimental data. It confirms a hypothesis that explains qualitative variation of the spectral dependences of T of the composites with the randomly inclined nanowires (namely, reduction of the T value and disappearance of its frequency dispersion) by development of the anisotropic network therein.

Conclusions

The composites with the metal nanowires, the transmittance T of which is dependent on the polarization of incident terahertz radiation, were produced on the track-etched membranes basis. It was demonstrated by comparing the transmission spectra of the samples with the different geometry of nanowires within the range 0.1–1 THz that this dependence is related to an anisotropic distribution of the nanowires in the composite, namely, their angular distribution. Thus, the composites that contain the nanowires inclined to the membrane plane are characterized by the dependence of the electromagnetic response on polarization of THz radiation, whereas a response of the

composites with the nanowires oriented strictly normal to the membrane plane does not depend on polarization. At the same time, the dependence on radiation polarization is most pronounced for the composites based on industrial track-etched membranes of the R geometry, since dispersion of NWs inclination within $\pm 30^\circ$ along one of the axes of the membrane plane results in formation of electrical contacts between the nanowires and gradual development of the conductive percolation network in the composite. The hypothesis stating that it is electrical percolation in the R-samples that is responsible for reduction of the absolute value of the transmittance and an increase of the polarization degree for such samples, is confirmed by compliance of the experimentally observed and theoretically obtained values of the NW lengths, at which the percolation transition is observed. Within the studied frequency range, the values of the polarization degree for such composites achieve 90%, while for the composites that contain parallel nanowires oriented strictly at the angle of 43.5° to the membrane surface, the polarization degree significantly depends on the frequency and does not exceed 6%.

The results of the study allow us to tell that it is promising to develop polarizers, attenuators and other optical elements based on the composites with oriented nanowires, for generating, converting and detecting terahertz-frequency radiation.

Acknowledgments

The authors would like to thank P.Yu. Apel (JINR, Dubna) for providing the samples of the various-type membranes and V.V. Artemov (KI, Moscow) for the SEM studies.

Funding

The experimental samples were synthesized under the state assignment of NRC „Kurchatov Institute“, the experimental part of the study was performed with support of a grant of the Belarusian Republican Foundation for Fundamental Research No. F24M-013, and the numerical models for calculating the percolation phenomena in the composite materials were developed with support of a grant of the Belarusian Republican Foundation for Fundamental Research F26RNF-043.

Conflict of interest

The authors declare that they have no conflict of interest.

References

- [1] A.A. Mashentseva, D.S. Sutekin, S.R. Rakisheva, M. Barsbay. *Polymers*, **16** (18), Art. N 18 (2024). DOI: 10.3390/polym16182616
- [2] N. Parsa, R.C. Toonen. *IEEE Nanotechnology Magazine*, **12** (4), 28 (2018). DOI: 10.1109/MNANO.2018.2869234

- [3] J. Xu, J. Zhang, J. Wang, Bo Hong, X. Peng, X. Wang, H. Ge, J. Hu. *J. Magn. Magn. Mater.*, **499**, 166207 (2020). DOI: 10.1016/j.jmmm.2019.166207
- [4] P. Apel. *Radiation Measurements*, **34** (1–6), 559 (2001).
- [5] F. Liu, M. Wang, X. Wang, P. Wang, W. Shen, S. Ding, Yu. Wang. *Nanotechnology*, **30** (5), 052001 (2018). DOI: 10.1088/1361-6528/aaed6d
- [6] S.J. Boehm, L. Kang, D.H. Werner, C.D. Keating. *Adv. Funct. Mater.*, **27** (5), 1604703 (2017). DOI: 10.1002/adfm.201604703
- [7] E.E. Evans, A.R. Shields, R.L. Carroll, S. Washburn, M.R. Falvo, R. Superfine. *Nano Lett.*, **7** (5), 1428 (2007). DOI: 10.1021/nl070190c
- [8] E. Kozhina, S. Bedin, A. Martynov, S. Andreev, A. Piryazev, Yu. Grigoriev, Yu. Gorbunova, A. Naumov. *Biosensors*, **13** (1), 46 (2022). DOI: 10.3390/bios13010046
- [9] M.R.Z. Kouhpanji, B.J.H. Stadler. *Sensors*, **21** (13), Art. N 13 (2021). DOI: 10.3390/s21134573
- [10] D.L. Zagorskiy, I.M. Doludenko, S.G. Chigarev, E.A. Vilkov, V.M. Kanevskii, A.I. Panas. *IEEE Trans. Magn.*, **58** (2), 1 (2022). DOI: 10.1109/TMAG.2021.3083407
- [11] C. Mijangos, R. Hernández, J. Martin. *arXiv:1706.08069*. DOI: 10.48550/arXiv.1706.08069
- [12] D.S. Bychanok, M.V. Shuba, P.P. Kuzhir, S.A. Maksimenko, V.V. Kubarev, M.A. Kanygin, O.V. Sedelnikova, L.G. Bulusheva, A.V. Okotrub. *J. Appl. Phys.*, **114** (11), 114304 (2013). DOI: 10.1063/1.4821773
- [13] X. Jiang, H. Yu, H. Lu, Y. Si, Yu. Dong, Ya. Zhu, Ch. Qian, Ya. Fu. *ACS Appl. Polym. Mater.*, **5** (6) 4400 (2023). DOI: 10.1021/acsapm.3c00518
- [14] M.V. Shuba, D.I. Yuko, G. Gorokhov, D. Meisak, D.S. Bychanok, P.P. Kuzhir, S.A. Maksimenko, P. Angelova, E. Ivanov, R. Kotsilkova. *Mater. Res. Express*, **6** (9), 095050 (2019). DOI: 10.1088/2053-1591/ab2edf
- [15] D. Zagorskiy, I. Doludenko, O. Zhigalina, D. Khmelenin, V. Kanevskiy. *Membranes*, **12** (2), 195 (2022). DOI: 10.3390/membranes12020195
- [16] A.V. Eletsii, A.A. Knizhnik, B.V. Potapkin, J.M. Kenny. *Physics-Uspekhi*, **58** (3), 209 (2015). DOI: 10.3367/UFNe.0185.201503a.0225
- [17] M.A. Kazakova, G.V. Golubtsov, A.G. Selyutin, A.V. Ishchenko, A.N. Serkova, G.V. Gorokhov, Ph.Y. Misiyuk, N.I. Valynets. *Mater. Chem. Phys.*, **307**, 128176 (2023). DOI: 10.1016/j.matchemphys.2023.128176
- [18] T. Sasaki, H. Okuyama, M. Sakamoto, K. Noda, H. Okamoto, N. Kawatsuki, H. Ono. *J. Appl. Phys.*, **121** (14), 143106 (2017). DOI: 10.1063/1.4981244
- [19] J. Kyoung, E.Yu. Jang, M.D. Lima, H.-R. Park, R.O. Robles, X. Lepró, Yo.H. Kim, R.H. Baughman, D.-S. Kim. *Nano Lett.*, **11** (10), 4227 (2011). DOI: 10.1021/nl202214y
- [20] B. Chen, X. Fu, X. Liu, Yo. Pan, S. Dong, B. Wang, Zh. Lin, H. Jiang. *Photonics*, **12** (11), 1046 (2025). DOI: 10.3390/photonics12111046
- [21] M.V. Shuba, A.V. Melnikov, A.G. Paddubskaya, P.P. Kuzhir, S.A. Maksimenko, C. Thomsen. *Phys. Rev. B*, **88** (4), 045436 (2013). DOI: 10.1103/PhysRevB.88.045436
- [22] G.Ya. Slepian, M.V. Shuba, S.A. Maksimenko, C. Thomsen, A. Lakhtakia. *Phys. Rev. B*, **81** (20), 205423 (2010). DOI: 10.1103/PhysRevB.81.205423
- [23] D. Zhu, M. Bosman, J.K.W. Yang. *Opt. Express*, **22** (8), 9809 (2014). DOI: 10.1364/OE.22.009809
- [24] H. Gu. *AM*, **5** (1), 1 (2016). DOI: 10.11648/j.am.20160501.11
- [25] P.Y. Apel. *Mater. Chem. Phys.*, **339**, 130681 (2025). DOI: 10.1016/j.matchemphys.2025.130681

Translated by M.Shevelev